Modeling Ammonia and Water Co-Adsorption in CuI-SSZ-13 Zeolite Using DFT Calculations

Hugo Petitjean, Céline Chizallet, Dorothée Berthomieu

Modeling Ammonia and Water co-Adsorption in Cu^{I}-SSZ-13 Zeolite Using DFT Calculations

Hugo Petitjean[1], Céline Chizallet[2] and Dorothée Berthomieu[1]*

[1]Institut Charles Gerhardt Montpellier, UMR 5253 CNRS-ENSCM-UM, Montpellier, France

[2]IFP Energies Nouvelles, Rond-point de l'échangeur de Solaize, BP3, 69360 Solaize, France

Corresponding author: dorothee.berthomieu@enscm.fr

ABSTRACT:

Cu-SSZ-13 efficiently catalyzes the selective catalytic reduction (SCR) of NO by NH_3 but the structure of the active site and, particularly, the redox state of the copper (+I or +II) are still debated. This paper focuses on the possible contribution of Cu^I species with a theoretical investigation of adsorption and co-adsorption of NH_3 and H_2O on Cu^I species using quantum chemistry and including dispersion forces. The calculations show that Cu^I clearly migrates upon adsorption of NH_3. While Cu^I is initially in close interaction with the zeolite framework, it preferentially forms coordination bonds with NH_3 and interacts with the zeolite in its second coordination sphere. The same tendency is calculated with H_2O, even if the binding energy of H_2O with Cu^I is lower than with NH_3. All the Cu^I complexes sit in the cage containing the 8 MR. The confined Cu^I complexes interact with the zeolite framework through several H-bonds donated by the NH or OH bonds of the ligands. In the experimental temperature and pressure domain of SCR conditions, calculated phase diagrams show that coordination number of two is predicted for the co-adsorption of NH_3 and H_2O on Cu^I. For pure H_2O, few stable domains for hydrated species containing Cu^I are calculated in contrast with pure NH_3. Finally, the calculated phase diagrams on Cu^I-SSZ-13 are discussed together with the more documented diagrams of Cu^{II}-SSZ-13 and recent experimental characterizations, providing a wider picture of the real catalyst in SCR conditions.

ORCID

D. Berthomieu: 0000-0002-3818-105X

C. Chizallet: 0000-0001-5140-8397

1. INTRODUCTION

Transition metal ions form coordination complexes with nuclearities and geometries depending on the coordination preference and oxidation state of the metal, and on the number, nature and affinity of the ligands. Exchanging transition metal ion in zeolites provides a class of very efficient catalysts.[1-2] Cu-exchanged zeolites and, particularly, Cu-SSZ-13 were reported as some of the most active catalysts[3-7] for the selective catalytic reduction (SCR) of NO_x by NH_3 or hydrocarbons.[8-11] The development of such materials requires a better understanding of the reaction mechanisms and a deeper knowledge of zeolite structures in the presence of hosted molecules. Thus, the structure of the catalysts and the evolution of the active species during the catalytic reactions have been analyzed with in situ/operando spectroscopies such as IR, X-ray Absorption Spectroscopies (XAS) and X-ray Emission Spectroscopies (XES).[6, 12-18] The spectroscopic signals are most generally assigned using reference compounds and computational chemistry, in an iterative process. Such strategies provided indications that isolated redox $Cu^{I/II}$ species are active sites in the Cu-SSZ-13 catalyst and provided geometric structures, oxidation states, and structure evolutions of the catalysts during SCR of NO by NH3.[12, 14, 19-25] There are strong spectroscopic indications that the valence state, the coordination and the position of the copper metal active site change upon addition of reactants and formation of products during the SCR of NO by NH_3 on Cu-SSZ-13 catalyst. However, the relationship between the spectroscopic signatures and the structure of the copper species in Cu-SSZ-13 is not straightforward. There is still a debate concerning the location, the coordination number (CN) and the oxidation state of Cu in Cu-SSZ-13 during SCR of NO by NH_3. Among the computational chemistry methods,

Density Functional Theory-based quantum chemistry is one of the most accurate and useful method to describe material structures containing transition metal ions. It allows predicting how the metal active site structure evolves upon addition of the reactants. Providing very accurate data for materials, DFT-based quantum modeling has to be considered as a theoretical tool to predict solid properties or as a complement of spectroscopic experimental data.[22-23, 26]

The adsorption of gas molecules in solid porous catalyst is an essential step in heterogeneous catalysis and the present theoretical study focuses on the adsorption of both H_2O and NH_3 on the Cu-SSZ-13 catalyst. Indeed the SCR of NO by NH_3 leads to the formation of H_2O and both are strong ligands interacting with copper. Earlier spectroscopic studies of Cu-SSZ-13 upon NH_3 adsorption on Cu revealed the presence of linear Cu^I species, O-Cu-NH_3 and NH_3-Cu-NH_3.[13, 17] Earlier studies on the impact of the addition of NH_3 and H_2O on Cu^I-exchanged zeolite using experiments combined with quantum chemistry clearly indicated that a migration of Cu^I may occur upon addition of reactants.[13, 17] Such migrations were reported, in particular for Cu^{II},[19, 26] and for $Cu^{I/II}$-SSZ-13 without adsorbent or in the presence of adsorbents.[14, 24, 27-29] While a lot of studies were devoted to Cu^{II}, few of them considered Cu^I. To advance our understanding about SCR with NH_3 on Cu-SSZ-13, a detailed analysis of the adsorption of water and co-adsorption of both NH_3 and water on Cu^I-SSZ-13 is required. The present theoretical investigation aims at describing the position and the coordination structure of Cu^I in SSZ-13 upon co-adsorption of the two strong ligands involved in SCR, H_2O and NH_3. To account for the SSZ-13 zeolite framework, periodic unit cells were considered. Based on a recent theoretical study on hydrated Cu^I clusters,[30] showing a preference for low coordinated structures, the number of NH_3 and H_2O ligands were limited to four, to calculate the co-adsorption phase diagrams using DFT. This

choice was also motivated by the well-known decrease of the coordination numbers (CN) from Cu^{II} to Cu^{I} in Cu-SSZ-13.[14, 24, 31]

We aim at clarifying the Cu^{I} species relevant in the experimental conditions used for SCR of NO by NH_3 in Cu^{I}-SSZ-13. The final discussion of the paper revisits the interpretation of recent operando EXAFS experiments in the light of phase diagrams calculated here and in previous studies[32] to describe the stable copper species in the experimental temperature (basically, between 450 and 623 K)[21] and pressure domains of the SCR.

2. COMPUTATIONAL METHODS

2.1. Models

Zeolite SSZ-13 has a chabazite (CHA) structure. It contains 4, 6 and 8 MR (Membered Rings) leading to the formation of large ellipsoidal cages with access through 8MR. Two ellipsoidal cages are connected by a prism cage called D6MR (Double Six Membered Rings). Such arrangement leads to the formation of large windows through 8MR.

A periodic unit cell of SSZ-13 with $O_{24}Si_{11}Al_1$ formula was considered, e.g. a Si/Al ratio of 11. The negative charge induced by the presence of one Al was compensated by one Cu^{I} in order to obtain material charge neutrality (Cu/Al=1). All the SiO_4 tetrahedra being equivalent, one Si from the 12 Si was exchanged for one Al. Each tetrahedron involves four non-equivalent O atoms labelled O_1, O_2, O_3 and O_4 as shown in Figure 1:[33-34] O adjoining two 4MR, one of the two 4MR being involved in a D6MR, is labelled O_1; O adjoining one 4MR and one 8MR is labelled O_2; O adjoining one 4MR of a D6MR, one 6MR of the D6MR and one 8MR is labelled O_3; and O adjoining two 4MR and one 6MR from a D6MR is labelled O_4.

Among all the crystallographic positions for exchanged cations in CHA structure[33-34] only those accessible to reactants e.g. in the largest cages were considered for copper: these sites are labelled sites I, IV and IV' (Figure 1). Site I is at the center of a 6MR from a D6MR along the [111] direction labelled using the dashed dotted black line in Figure 1. Each of these 6MR contains three O_4 and three O_3. At this position, a cation that occupies the center of a 6MR may have a three-fold coordination with three O atoms.

Site IV is located near a 8MR window with one O_1 and one O_2 oriented in the direction of site IV. Site labelled IV' is located near a 8MR window with two O atoms, O_2 and one O_3, directed to this position (Figure 1).

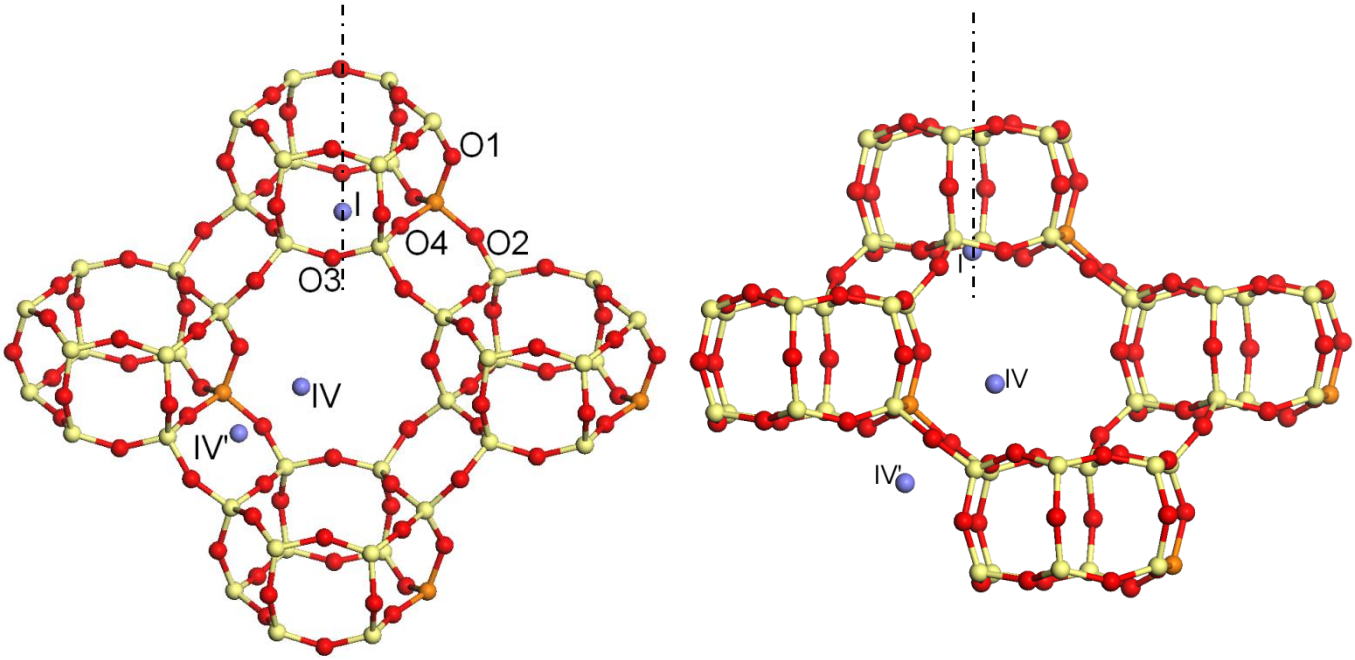

Figure 1. Labels of the framework oxygen atoms and the exchange site positions in the SSZ-13 model unit cell. Sites I are at the center of a 6MR, and sites IV and IV', near a 8MR. Red balls are O, yellow ball are Si, orange ball is Al, and exchange site positions are blue balls. Dashed dotted line is for the D6MR axis.

The geometries were fully optimized to compare the relative energy values of the Cu^{I}-SSZ-13 structures.

To calculate phase diagrams, the fully optimized structure $(NH_3)_2Cu^{I}$-SSZ-13 unit cell parameters were considered as a starting geometry for all the structures containing co-adsorbed ammonia and water and for all the structures containing ammonia or water only. The unit cell parameters (a=9.2968 Å, b=9.4111Å, c= 9.2282Å, α=93.34°, β=92.68° and γ=94.88°) were kept fixed while all atom positions were allowed to relax during geometry optimizations.

Free NH_3 and H_2O were optimized both using the present periodic unit cell and also using a molecular approach.

2.2. Methods

Calculations were performed with the hybrid B3LYP exchange-correlation functional,[35-36] using the massively parallel versions of the periodic *ab-initio* CRYSTAL09 and CRYSTAL14 codes.[37, 38] B3LYP includes exact Hartree-Fock exchange, which provides more accurate binding energy values in the modeling of copper complexes.[39] The electronic structures were computed with all-electron Gaussian basis sets: 6-311G(d) for H, N, Al, Si and O, and TZP 842111/631/4111 set for Cu.

The calculation method includes dispersion forces using empirical Grimme correction labelled D*[40-41] for the phase diagrams because it is required to reproduce coordination complex formation of Cu^{I} with four H_2O in the first coordination sphere of copper, as it is calculated with post-Hartree-Fock calculation methods.[30]

Geometry was optimized before frequency calculations with the following criteria: $4.5 \cdot 10^{-4}$ and $3 \cdot 10^{-4}$ a.u. for the gradient thresholds (resp. maximum and RMS), and $1.8 \cdot 10^{-3}$ and $1.2 \cdot 10^{-3}$ a.u.

for the displacement thresholds (resp. maximum and RMS). The integration grid is a pruned grid with 75 radial points and a maximum number of 974 angular points in regions relevant for chemical bonding (XLGRID keyword). The Brillouin zone was sampled with 8 reciprocal kpoints.

The Hessian matrices were calculated systematically for all the complexes to ensure that the geometries are minima on the potential energy surface. SCF convergence was set to 10^{-7} Hartree for the energy. Harmonic vibrational frequencies were calculated at the gamma point. Thermodynamic functions were calculated on the basis of statistical mechanics equations available in the CRYSTAL14 program.

The Gibbs free energies were calculated according to the approach detailed in ref.[32] by considering the rotational, translational, and vibrational degrees of freedom for gas-phase water and ammonia, and the vibrational degrees of freedom only for the zeolite models. The Gibbs free energy values were calculated at a temperature domain between 398 and 698 K and a pressure of 1 Atm.

The cumulated adsorption energies E of H_2O and NH_3 on Cu^I-SSZ-13 were calculated as the electronic energy difference E (equation (1)).

$$E = E[Cu^I(L)_x\text{-SSZ-13}] - E[Cu^I\text{-SSZ-13}] - xE[L] \qquad \text{Eq. (1)}$$

with $L=H_2O$, NH_3 and x, the number of ligands ($1 \leq x \leq 4$).

The configurations are labeled (n,m) with n and m the number of adsorbed H_2O and NH_3 molecules respectively, with $0 \leq n \leq 4$, $0 \leq m \leq 4$ and $0 \leq n+m \leq 4$.

All electronic energies of adsorption are corrected from basis set superposition error (BSSE) using correction terms for the energies of the free ligands, water and ammonia, after a thorough study of the counterpoise correction.[42] For all complexes, we evaluated the BSSE by calculating

the counterpoise correction for the interaction of each ligand with copper in the complex. For instance, with the adsorption structure (2,2), we calculated the four terms of the counterpoise correction for each of the four ligands (e. g. 16 SCF energy calculations) in interaction with the complex of copper coordinated with the three other ligands in the zeolite. From all these calculations, we evaluated the energy differences when the wavefunction of the partner (ligand or complementary complex) is calculated with its own basis functions or with the full set available in the adsorption structure. Considering all the adsorption structures, for the partner water, the addition of the ghost functions at fixed geometry lowers the energy by 20 ± 5 $kJ.mol^{-1}$; for ammonia, 35 ±5 $kJ.mol^{-1}$; and for the coordinated copper, 18 ±7 $kJ.mol^{-1}$. As previously reported[43] and confirmed here, the stabilization due to the ghost functions strongly depends on the environment of the partners in interaction. In the present case, the counterpoise correction seems delicate to be applied as usual for two main reasons: firstly, from an adsorption complex to another, the coordination geometry of the copper complex changed dramatically and secondly, the complexes are stabilized with several versatile H-bonds between oxygen atoms of the zeolite framework and the O-H/N-H bonds of the ligands. As the counterpoise correction is known as overestimating the BSSE, we included only part of the counterpoise correction in order to describe the ligand exchange more accurately. As a compromise solution, we neglected the contribution from the coordinated copper part. From our methodical study of the stabilization terms, we assigned an average correction for the energy of the free ligands: -20 $kJ.mol^{-1}$ for free water and -35 $kJ.mol^{-1}$ for free ammonia.

A special attention was paid to investigate the structures of complexes after the addition of 2 NH_3 molecules in Cu^{I}-SSZ-13[24, 44] because a series of BOMD (Born Oppenheimer Molecular Dynamics) simulations at 300 K provided large changes of the initial Cu^{I} in the zeolite

framework and coordination numbers (CN), consistent with experiments and modelings. BOMD simulations were used as a tool to investigate deeply the potential energy surface for the (0,2) combination. Then geometry optimizations were performed. The two NH_3 molecules were initially located in the first coordination sphere of optimized Cu^I-SSZ-13 structures. Then, the most stable optimized structure with 2 NH_3 molecules in Cu^I-SSZ-13 (e.g. (0,2) combination) was used as starting point for increasing or decreasing the loading of NH_3 in the first coordination sphere of Cu^I, and to generate structures with pure H_2O and structures containing both NH_3 and H_2O. This strategy was used to generate the (n, m) combinations for the calculation of sequential desorption energies and Gibbs free energy diagrams.

3. RESULTS AND DISCUSSION

3. 1. *Cu-SSZ-13*

Geometry optimisation of Cu^I-SSZ-13 led to three structures, **A**, **B** and **C** with Cu^I located in three different positions in the largest cage (Figure 2). In agreement with previous DFT results,[45-46] the most stable structure **A** has a Cu^I at site I while the less stable structure **C** has a Cu at site IV'.[33-34] The intermediate structure **B** has a Cu at site IV (Table 1).

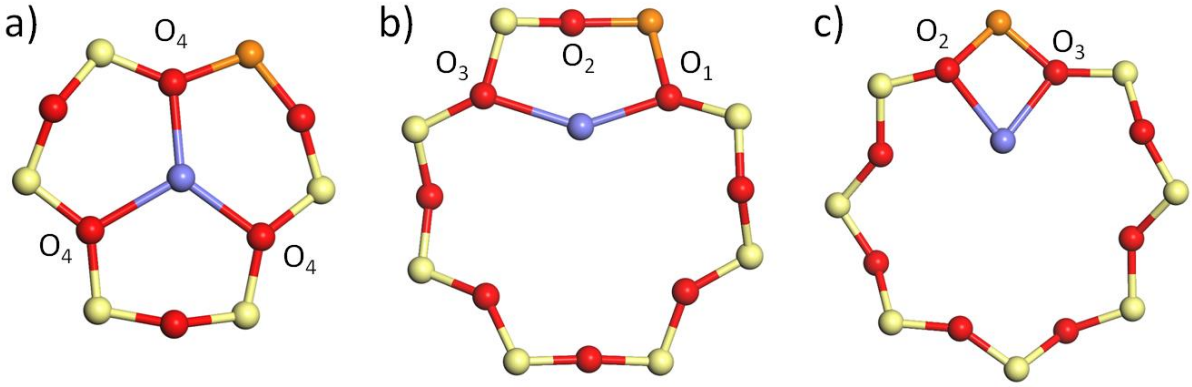

Figure 2. Cu^{I} in exchange positions in SSZ-13: a) structure A with Cu^{I} in site I, b) structure B with Cu^{I} in site IV, and c) structure B with Cu^{I} in site IV'. Red balls are O, yellow ball are Si, orange ball is Al, and exchange site positions are blue balls.

These three geometries exhibit strong similarities with previously calculated structures.45-46 The relative energy between structure A and structure B (43 kJ.mol-1) is very similar to the value of 40.5 kJ.mol-1 previously calculated with a periodic B3LYP method, including a posteriori correction of the long range dispersion.46 Structure C containing CuI at site IV' has a relative energy value of 54 kJ.mol-1 (Table 1). It is thus less stable than the structures with Cu at site I or IV.

The most stable structure A corresponds to CuI with CN of 3 (defined as the number of heavy atoms within 2.3 Å of Cu as in ref.24). In CuI-SSZ-13, the three O4 directed to the center of the 6MR led to the smallest Cu-O bonds, while the three other O3 atoms were directed to the 8MR with largest Cu-O bonds. As reported with other mononuclear cations in 6MR of zeolites,47 the ring is slightly distorted after optimization because the presence of one Al tetrahedron in the 6MR induces a dissymmetry, leading to larger Al-O bond lengths and O-Al-O angles in comparison with Si-O and O-Si-O (Table S2). The CN of 3 computed for the structure A is in line with previous modeling studies of zeolites with monocation exchanged in 6MR,2, 24-25, 48 in particular using static calculations for CuI at site I of chabazite.45-46 However recent studies including Ab Initio Molecular Dynamics evidenced many minima with CN of 2 or 3 on the potential energy surface for CuI in the 6MR of the SSZ-13 zeolite.27,24 Such approach goes in the direction of the high mobility experimentally demonstrated for CuI in the SSZ-13 unit cell changing its coordination, and responsible for a CN, between 2 and 3.

In the two less stable optimized structures, CuI is in the 8MR, coordinated to O1 and O3 in B (O2 is further than the cut-off distance of 2.3 Å used to define the CN), and to O3 and O2 in C, both with CN of 2. The short Cu-O bonds induce a strong deformation of the 8MR as reflected in the O2-Al-O4 angle of 100° and O4-Si-O1 angle of 104° in B that decrease to O2-Al-O4 angle of 98° and increases to O4-Si-O1 of 106° in C. These changes in the copper interaction with the SSZ-13 framework in B and C, in comparison with A, are most probably responsible for the stability decrease.

In the absence of chemisorbed molecule in the first coordination sphere of CuI, the most stable structure contains CuI at site I with a CN of 3 in contrast with an expected CN of 2 from experiment, and in contrast to the experimental proposal of CuI positioned in two different sites based on H2-TPR and FTIR studies.6 Recent calculations report different coordination of CuI at site I in the D6MR.24, 27 These differences reveal that most probably the Potential Energy Surface (PES) for CuI in SSZ-13 contains several minima, as already shown in ref.23 Thus, at finite temperature, the structures B and C with CN of 2 that we calculated for CuI in 8MR could play a role and we decided to include the three structures in the thorough study of the ammonia adsorption, even if the energy differences between A, B and C are large.

3. 2. Addition of pure NH3 and H2O in Cu-SSZ-13

As the linear dicoordinated complexes of CuI are particularly stable, we started the modeling of adsorption with a deep investigation of the PES for the formation of (NH3)2-CuI-SSZ-13. From the three structures A, B and C, the addition of two NH3 molecules in the first coordination sphere of CuI led to several minima. Figure 2 shows the most stable X, Y and Z

optimized geometries (see Table S3 for the geometric parameters). Note that all other structures (for different adsorption stoichiometries) are reported in figure S1.

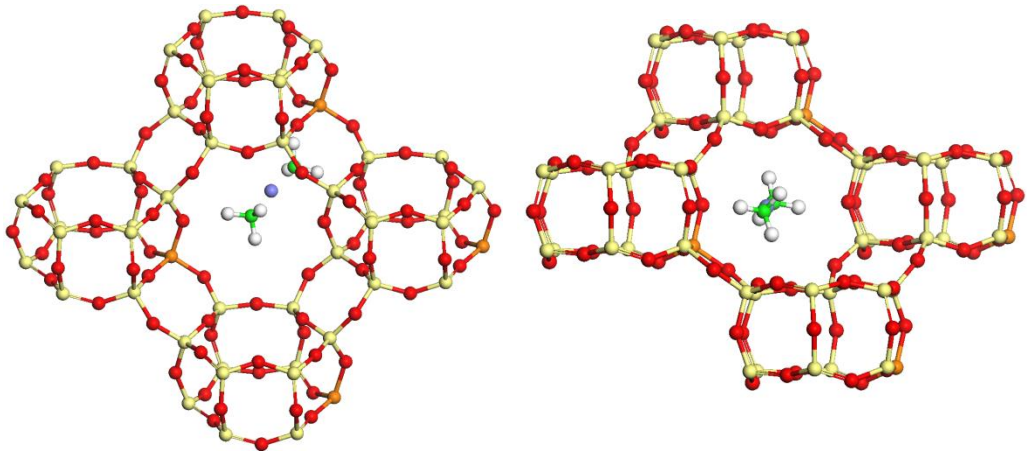

X

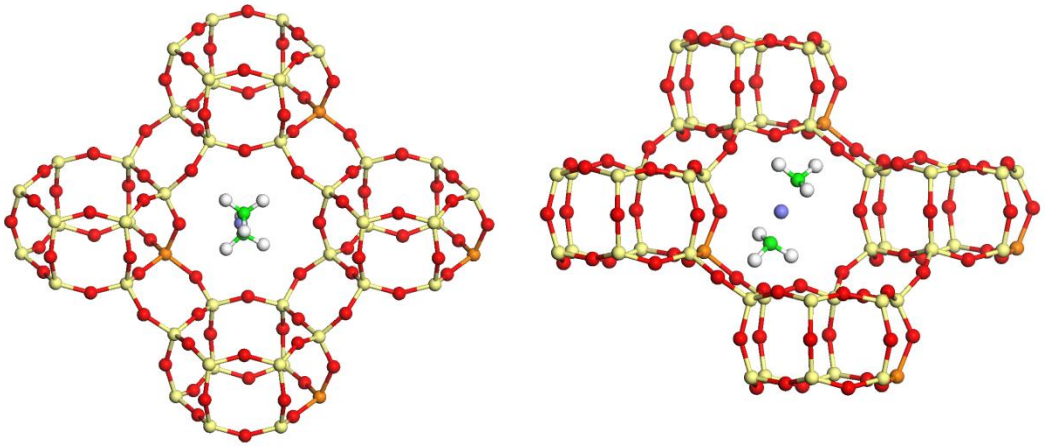

Y

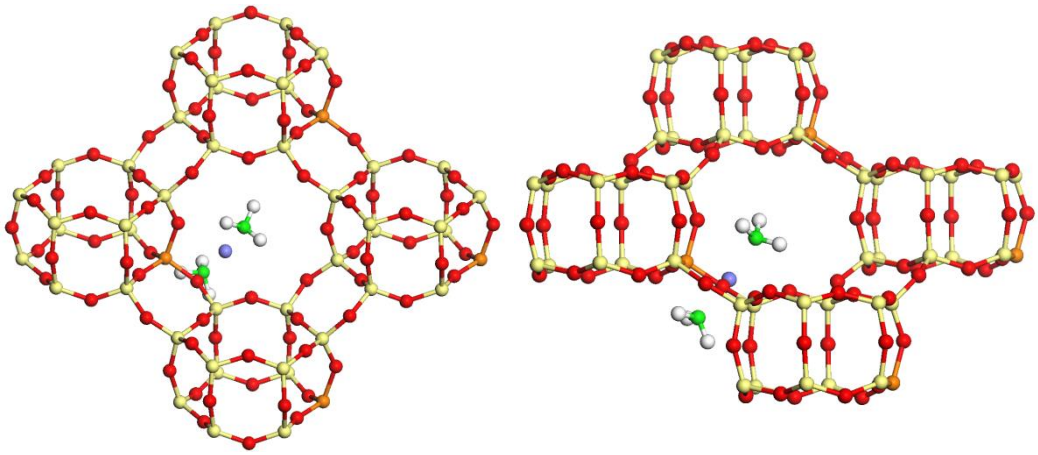

Z

Figure 3. Adsorption structures of 2 NH_3 in Cu^I-SSZ-13 unit cell: views of the three optimized structures **X**, **Y** and **Z**. Red balls are O, yellow ball are Si, orange ball is Al, green are N and blue ball are Cu^I.

Upon addition of two NH3 molecules, copper exchanges its framework oxygen ligands with NH3 ligands and moves toward the 8MR window of the SSZ-13. In the three most stable optimized geometries X, Y and Z, CuI gets far away from the zeolite walls and interacts with the zeolite through its second coordination sphere. This is illustrated by a significant increase of the Cu...Al bond distance larger than 3 Å. For the three geometries, copper is twofold-coordinated to two NH3 molecules (Table S3) with Cu-N below 2 Å. The energy difference between the two most stable structures X and Y is 19 kJ.mol-1 using B3LYP (Table S3). This is significantly smaller than the energy difference of 43 kJ.mol-1 between the structures A and B without NH3 (Table S1).

The most stable structure is the X structure, as already reported.17, 49 In structure X, the two short Cu-N bonds are of around 1.94 Å, in agreement with recent computational results.24 The N-Cu-N angle (calculated below 176°) is rather linear, in line with a two-fold coordination. Each

of the two NH3 molecules establishes a short hydrogen bond with oxygen atoms of the zeolite framework (H...O distance of 2.03 and 1.95 Å respectively).

The addition of two H2O molecules in CuI-SSZ-13 led to a structure very similar to the structure X calculated with NH3, CuI is located in the 8MR and has a CN of 2. Each of the two H2O molecule has at least one H..O bond length distance with O from the zeolite framework below 2 Å. The O-Cu-O angle is below 171°, in line with a linear O-Cu-O structure.

The addition of 3 and 4 NH3 in the first coordination sphere of CuI follows the behavior evidenced with the diammino complex. CuI remains in the 8MR window and adopts structures without any symmetry (nor C2v, nor Td for (0,3) and (0,4) configurations, respectively). Each NH3 has at least one short H...O distance with O from the zeolite framework, depicting the existence of hydrogen bonds. Qualitatively similar results are obtained for the addition of 3 and 4 H2O molecules.

Finally, we studied the unfavorable addition of one molecule per CuI site to fully describe the adsorption scheme. The addition of one NH3 in CuI-SSZ-13 leads to the formation of a complex with CuI and NH3 located in the 8MR and close the O4 atom of the Al tetrahedron in the 6MR, with a Cu-O4 bond length in the range of 1.98 Å, similar to the Cu-N bond length, a Cu...Al distance in the range of 4.4 Å and a O-Cu-N angle in the range of 160°. This structure is slightly different from the previous reported structure having a short Cu...Al distance in the range of 2.78Å.24

Similarly to the adsorption of one NH3, the adsorption of one H2O induces a displacement of CuI in the 8MR in SSZ-13. The formation of a complex with CuI and H2O located in the 8MR and close the O3 atom of Si tetrahedra in the 6MR was calculated. A Cu-O bond length in the range of 2.01 Å different to the Cu-O bond length of 1.91 Å, a Cu...Al distance in the range of

4.28 Å and an O3-Cu-O angle in the range of 172° and the two H atoms very close to two O atoms from the zeolite framework (bond distances below 2 Å: 1.78 and 1.98 Å) were computed. Present structure is different from the previous reported structure having a O3-Cu-O angle in the range of 172° and a O4-Cu-O angle in the range of 97° and a short Cu...Al distance in the range of 2.79 Å.24 The difference between the two structures are in line with a flat PES that may contain several minima, as previously reported.14

Figure 4 shows the B3LYP-D* cumulated adsorption energies of H2O and NH3 respectively on CuI-SSZ-13 (exact values in Table S4). The present NH3 and H2O adsorption energy values are smaller than previous reported values, most probably because the present quantum calculation method is different and because the calculated configurations exhibit different structures, in contrast with previous studies.14, 22, 24, 28, 45

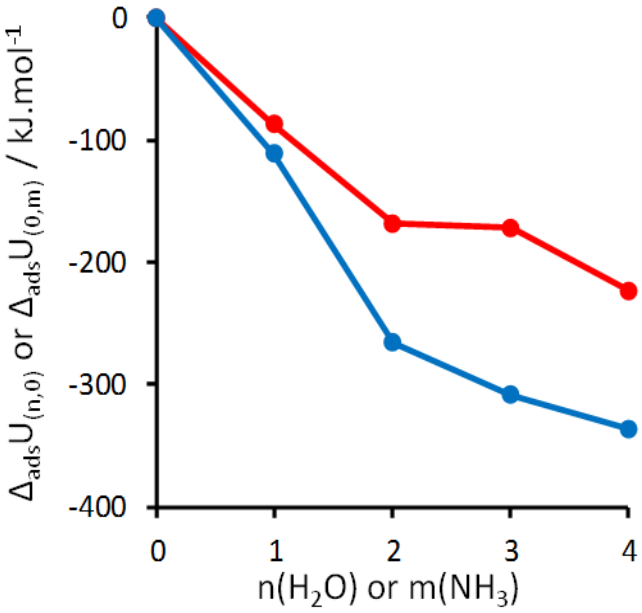

Figure 4. Adsorption of H_2O or NH_3 on Cu^I-SSZ-13: cumulated adsorption energies of n H_2O (red line) or m NH_3 (blue line) on Cu^I-SSZ-13 complexes (n being the number of water molecules and m, the number of ammonia molecules per Cu^I).

As expected with Cu^{I}, the ammino complexes are much more stable than the aquo complexes. In comparison with Cu^{II}-SSZ-13,[24, 32] the cumulated adsorption energies are similar for one or two ligand molecules but they stagnate when further molecules are coordinated: for Cu^{I}-SSZ-13, the complexes with 2 molecules (linear dicoordinated structures) are particularly stable, whereas higher coordinated species are stable for Cu^{II}.

3. 3. *Co-adsorption of NH_3 and H_2O on Cu-SSZ-13*

The energy diagrams of the co-adsorptions of NH_3 and H_2O were calculated from addition (or elimination) of ammonia and water ligands (L) on the **X** structure. All the combinations were optimized for NH_3 and H_2O and only the most stable structures are reported (Table S5, Figure S1). Whatever the configurations, Cu^{I} is located in the 8MR window. The Cu...Al distance varies in a large extent from 3.38 to 4.96 Å, evidencing that, upon adsorption of water and/or ammonia, copper complexes move a lot in the channel containing the 8MR, either in position or in orientation.

The (n,m) configurations were used to build the thermodynamic stability domains of the adsorption of NH_3 and H_2O with respect to NH_3 and H_2O partial pressure, respectively. The phase diagrams for pure NH_3 and H_2O are given in Figure 5.

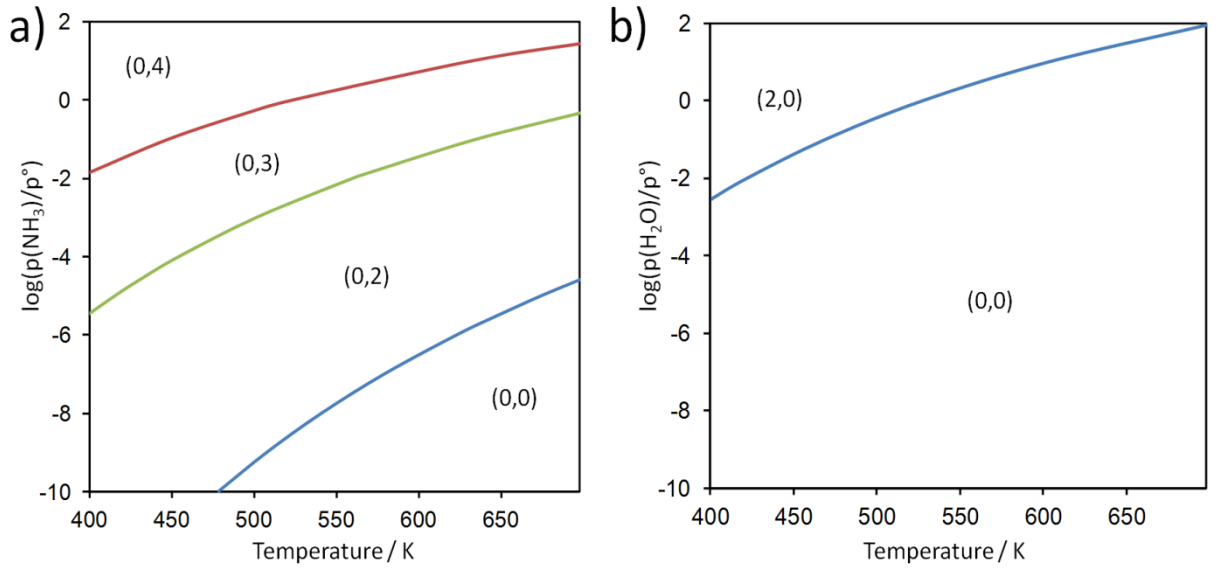

Figure 5. Phase diagrams of Cu^{I}-SSZ-13 in presence of ammonia or water: a) pure NH_3 adsorption on Cu^{I}-SSZ-13, (b) pure H_2O adsorption on Cu^{I}-SSZ-13. The (n,m) couple in each stability domain gives the number of water molecules (n) and the number of ammonia molecules (m) per Cu^{I}. Calculated with the B3LYP-D* functional and a compensation accounting for the BSSE.

The predicted phase diagram for pure NH3 exhibits similar tendencies to the one recently calculated49 except that the (0,1) configuration is absent in the present study and the stability domain for the (0,2) configuration is larger using B3LYP-D* as done in the present study.

The predicted phase diagram for pure H2O indicates very few stability domains, whit only one configuration (2,0) that would exist in the range of experimental SCR conditions. Different phase diagram, with (0,0) and (1,0) configurations only, was calculated in the presence of pressure of O2, thus accounting for the possible transformation of CuI into CuII.24

Finally, the phase diagram for the co-adsorption of NH3 and H2O (at p(H2O) = 10-2 bar and at p(NH3) = 10-3 bar) in Figure 6 (a) indicates that the stability domains are very similar at low

pressure of water and without water. This result illustrates the dominant role of ammonia with respect to water, which is also quasi absent from the CuII-SSZ-13 diagram using similar representation conditions reported in ref.32

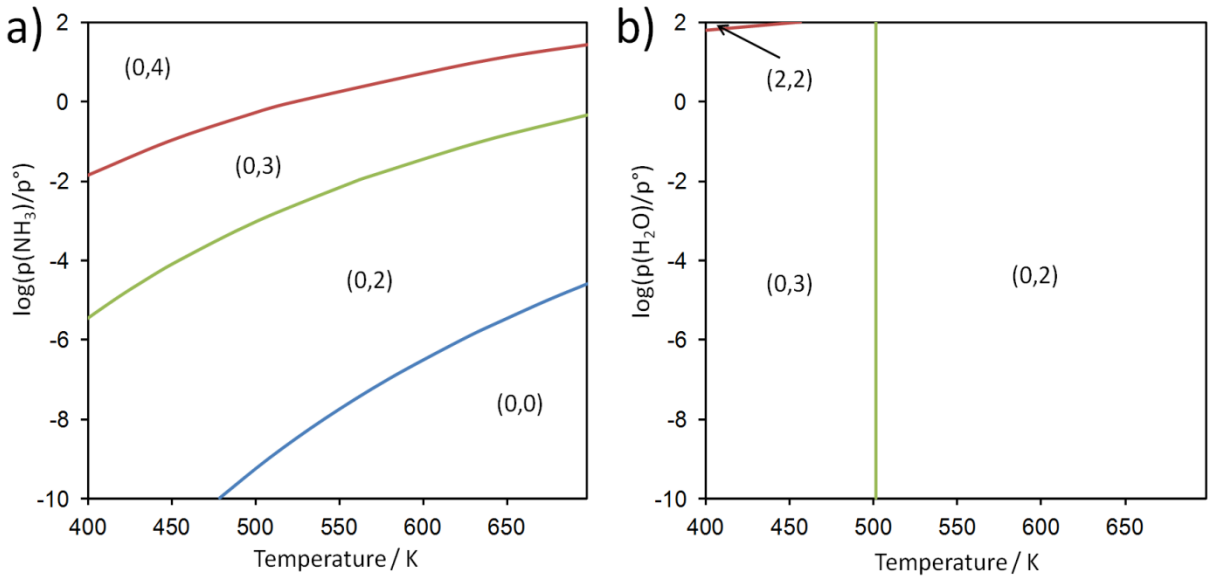

Figure 6. Phase diagrams of co-adsorption of NH_3 and H_2O on Cu^I-SSZ-13, for (a) $p(H_2O) = 10^{-2}$ bar and (b) $p(NH_3) = 10^{-3}$ bar. The (n,m) couple in each stability domain gives the number of water molecules (n) and the number of ammonia molecules (m) per Cu^I. Calculated with the B3LYP-D* functional and a compensation accounting for the BSSE.

According to the calculated phase diagrams, there is no stable domain for the adsorption of one NH_3 nor for one H_2O in Cu^I-SSZ-13. This result differs from the recent results for NH_3[49] and for H_2O.[24] The 14 calculated (n,m) configurations (Table S5) indicate that Cu^I is surrounded by H_2O/NH_3 in its first coordination sphere sites in the channel containing the 8MR where its CN is calculated between 4 and 1. According to the calculated energy diagrams for the co-adsorption of NH_3 and H_2O on Cu^I-SSZ-13, a CN of 2 is predicted, above 500K and below 500 K (Figure 6) at

a pressure of water above 60 bars. At low pressure of water and below 500K, a (0,3) configuration with a CN of 3 is predicted.

The calculated phase diagrams for SSZ-13 exchanged with Cu^{I} (present study) and Cu^{II} (ref.[32]) are used in the following discussion to better understand how the copper CN evolves in the experimental conditions. We will focus on the treatment of the Cu-SSZ-13 catalyst before the SCR experiments, and more precisely on the two first steps: the thermal dehydration of the copper-exchanged zeolite and the adsorption of ammonia.

To study the dehydration of the catalyst, Doronkin et al.[32] quantified by *in situ* EXAFS the evolution of the CN of copper as a function of the dehydration temperature, for an estimated residual partial pressure of 10^{-5} bar. According to the thermodynamic diagram shown in Figure 5-(b), in these conditions Cu^{I} is always adsorbate-free, so that its CN is expected to be constant at three (the three ligands being framework oxygen atoms). This means that the thermal evolution of the coordination number is mainly driven by the behavior of Cu^{II}, which was indeed explained by periodic ab initio calculations in ref.[32]. Experimentally, below 400 K the average CN of copper was close to 4.3 and dropped at 3.7 above 400 K, which is only partially rendered by the theoretical predictions made for Cu^{II}.[32] Indeed, considering the existence of Cu^{II} only does not explain the appearance of CN lower than 4 in these temperature conditions. Considering the co-existence between Cu^{II} (with CN = 4) and Cu^{I} species (with CN = 3) better explains this feature. Above 673 K experimentally, the CN of copper further drops at 3.0, which could only be explained by the predominance of Cu^{II} at the 8MR site in these conditions.[32] Now, such a CN is also compatible with the CN we quantify here for Cu^{I} free from adsorbates. Note however that the amount of Cu^{I} is likely very low in these dehydration conditions, considering the quasi-absence of the XANES features typical of Cu^{I} (prominent peak at the rising edge at 8983 eV).[32]

Adding ammonia in the feed (10^{-3} bar) was observed to promote the reduction of part of the Cu^{II} species into Cu^{I}, in agreement with previous findings,[29] in particular at increasing temperatures, and in the absence of water. When water was co-fed (10^{-2} bar) with ammonia, very similar trends were recorded for what regards ammonia retention, but the Cu^{II}/Cu^{I} ratio was affected, water acting as an inhibitor of the reduction by ammonia. In these conditions, our current calculations predict the same behavior of Cu^{I} whatever the presence or absence of water, with respect to the nature of the coordination sphere. This was also the case for Cu^{II}.[32] From EXAFS, the coordination number of copper decreases as the temperature increases, reaching a minimal value of 2 for a critical temperature that depends on the absence / presence of water, being equal to about 500 K / 623 K respectively. Our calculations for Cu^{I} predict the desorption of one ammonia molecule at 500 K in these conditions (Figure 6a), leading to a decrease of the coordination number from 3 to 2 (the ligands being ammonia molecules only, even for the highest temperatures sampled). This is in excellent agreement with the experimental observation made in the absence of water.[32] In the presence of water, the shift of the critical value at higher temperature (623 K) is compatible with a non-negligible role of Cu^{II} in these conditions. Altogether, the combined consideration of the thermal stability of Cu^{II} and Cu^{I} species thanks to the thermodynamic diagrams provides a unified view of the reactions taking place as a function of the temperature. Note however that according to our predictions, ammonia is expected to be present in the coordination sphere of Cu^{I}, whatever the temperature. This is in contradiction with Linear Combination Analysis of XANES spectra as provided in ref.[32] suggesting the dominance of such species above 673 K. We can indeed not exclude the existence of a distribution of species rather than the existence of a single one, our thermodynamic diagrams providing a very discrete insight in a phenomenon that is actually more statistical than depicted by the diagrams.

CONCLUSIONS

The present theoretical investigation aims at investigating configuration structures of mononuclear Cu^I in SSZ-13 zeolite involved in SCR catalytic reactions, through different NH_3 and H_2O pressures and different temperatures. Calculated structures using B3LYP functional and localized basis sets clearly show that in large pores containing 8MR, Cu^I is surrounded by NH_3/H_2O, with a strong preference for NH_3 in its first coordination sphere. The calculated cumulated adsorption energies clearly predict a regular decrease of the absolute adsorption energy values while the number of ligands in the first coordination shell of Cu^I decreases. The 8MR windows being large, the formation of complexes with different structures (minima) on the PES are most probably possible. The NH_3 and H_2O ligands facilitate the formation of H-bonds with O atoms from the zeolite framework and then contribute to the binding energies. Co-adsorption of NH_3 and H_2O provide complexes with a CN of two, only. Calculated phase diagrams clearly predict a preference for Cu^I solvated by 2 NH_3 above 500K, and for Cu^I solvated by 4 NH_3 below 500K or for Cu^I solvated by 2 NH_3 and 2 H_2O depending on the value of the pressure of water. Few stability domains are calculated for the adsorption of water on Cu^I in SSZ-13. These findings are of crucial help to rationalize experimental trends made for example by operando XAS.

ACKNOWLEDGMENTS

Pr. Dr. Claudio M. Zicovich-Wilson, Michel Rerat and Dr. Raffaella Demichelis are acknowledge for helpful discussions.

This work was performed using HPC resources from GENCI-[CCRT/CINES/IDRIS] (Grants No. 2010-x2011081071, A0010807394 and A0030807394).

REFERENCES

(1) Bell, A. T., Siting and stability of metal cations in zeolites. *NATO Sci. Ser., II* **2001,** *13*, 55-73.

(2) Berthomieu, D.; Delahay, G., Recent advances in CuI/IIY: experiments and modeling. *Catal. Rev. - Sci. Eng.* **2006,** *48* (3), 269-313.

(3) Beale, A. M.; Gao, F.; Lezcano-Gonzalez, I.; Peden, C. H. F.; Szanyi, J., Recent advances in automotive catalysis for NOx emission control by small-pore microporous materials. *Chem. Soc. Rev.* **2015,** *44*, 7371-7405.

(4) Dusselier, M.; Davis, M. E., Small-Pore Zeolites: Synthesis and Catalysis. *Chem. Rev. (Washington, DC, U. S.)* **2018,** *118*, 5265-5329.

(5) Kwak, J. H.; Tonkyn, R. G.; Kim, D. H.; Szanyi, J.; Peden, C. H. F., Excellent activity and selectivity of Cu-SSZ-13 in the selective catalytic reduction of NOx with NH3. *J. Catal.* **2010,** *275* (2), 187-190.

(6) Kwak, J. H.; Zhu, H.; Lee, J. H.; Peden, C. H. F.; Szanyi, J., Two different cationic positions in Cu-SSZ-13? *Chem. Commun.* **2012,** *48*, 4758-4760.

(7) Borfecchia, E.; Beato, P.; Svelle, S.; Olsbye, U.; Lamberti, C.; Bordiga, S., Cu-CHA - a model system for applied selective redox catalysis. *Chem. Soc. Rev.* **2018**, Ahead of Print.

(8) Iwamoto, M.; Furukawa, H.; Mine, Y.; Uemura, F.; Mikuriya, S.; Kagawa, S., Copper(II) ion-exchanged ZSM-5 zeolites as highly active catalysts for direct and continuous decomposition of nitrogen monoxide. *J. Chem. Soc., Chem. Commun.* **1986,** (16), 1272-3.

(9) Iwamoto, M.; Hamada, H., Removal of nitrogen monoxide from exhaust gases through novel catalytic processes. *Catal. Today* **1991,** *10* (1), 57-71.

(10) Iwamoto, M.; Yahiro, H.; Mizuno, N.; Zhang, W. X.; Mine, Y.; Furukawa, H.; Kagawa, S., Removal of nitrogen monoxide through a novel catalytic process. 2. Infrared study on surface reaction of nitrogen monoxide adsorbed on copper ion-exchanged ZSM-5 zeolites. *J. Phys. Chem.* **1992,** *96* (23), 9360-6.

(11) Iwamoto, M.; Yahiro, H.; Tanda, K.; Mizuno, N.; Mine, Y.; Kagawa, S., Removal of nitrogen monoxide through a novel catalytic process. 1. Decomposition on excessively copper-ion-exchanged ZSM-5 zeolites. *J. Phys. Chem.* **1991,** *95* (9), 3727-30.

(12) Guenter, T.; Carvalho, H. W. P.; Doronkin, D. E.; Sheppard, T.; Glatzel, P.; Atkins, A. J.; Rudolph, J.; Jacob, C. R.; Casapu, M.; Grunwaldt, J.-D., Structural snapshots of the SCR reaction mechanism on Cu-SSZ-13. *Chem. Commun.* **2015,** *51*, 9227-9230.

(13) Kwak, J. H.; Varga, T.; Peden, C. H. F.; Gao, F.; Hanson, J. C.; Szanyi, J., Following the movement of Cu ions in a SSZ-13 zeolite during dehydration, reduction and adsorption: A combined in situ TP-XRD, XANES/DRIFTS study. *J. Catal.* **2014,** *314*, 83-93.

(14) McEwen, J. S.; Anggara, T.; Schneider, W. F.; Kispersky, V. F.; Miller, J. T.; Delgass, W. N.; Ribeiro, F. H., Integrated operando X-ray absorption and DFT characterization of Cu-

SSZ-13 exchange sites during the selective catalytic reduction of NOx with NH3. *Catalysis Today* **2012,** *184* (1), 129-144.

(15) Zhang, R.; McEwen, J.-S., Local Environment Sensitivity of the Cu K-Edge XANES Features in Cu-SSZ-13: Analysis from First-Principles. *J. Phys. Chem. Lett.* **2018,** *9*, 3035-3042.

(16) Bordiga, S.; Groppo, E.; Agostini, G.; van Bokhoven, J. A.; Lamberti, C., Reactivity of Surface Species in Heterogeneous Catalysts Probed by In Situ X-ray Absorption Techniques. *Chem. Rev.* **2013,** *113*, 1736-1850.

(17) Giordanino, F.; Borfecchia, E.; Lomachenko, K. A.; Lazzarini, A.; Agostini, G.; Gallo, E.; Soldatov, A. V.; Beato, P.; Bordiga, S.; Lamberti, C., Interaction of NH3 with Cu-SSZ-13 Catalyst: A Complementary FTIR, XANES, and XES Study. *J. Phys. Chem. Lett.* **2014,** *5*, 1552-1559.

(18) Marberger, A.; Petrov, A. W.; Steiger, P.; Elsener, M.; Kröcher, O.; Nachtegaal, M.; Ferri, D., Time-resolved copper speciation during selective catalytic reduction of NO on Cu-SSZ-13. *Nature Catalysis* **2018,** *1* (3), 221-227.

(19) Andersen, C. W.; Borfecchia, E.; Bremholm, M.; Jorgensen, M. R. V.; Vennestrom, P. N. R.; Lamberti, C.; Lundegaard, L. F.; Iversen, B. B., Redox-Driven Migration of Copper Ions in the Cu-CHA Zeolite as Shown by the In Situ PXRD/XANES Technique. *Angew. Chem., Int. Ed.* **2017,** *56*, 10367-10372.

(20) Borfecchia, E.; Lomachenko, K. A.; Giordanino, F.; Falsig, H.; Beato, P.; Soldatov, A. V.; Bordiga, S.; Lamberti, C., Revisiting the nature of Cu sites in the activated Cu-SSZ-13 catalyst for SCR reaction. *Chem. Sci.* **2015,** *6*, 548-563.

(21) Deka, U.; Juhin, A.; Eilertsen, E. A.; Emerich, H.; Green, M. A.; Korhonen, S. T.; Weckhuysen, B. M.; Beale, A. M., Confirmation of Isolated Cu2+ Ions in SSZ-13 Zeolite as Active Sites in NH3-Selective Catalytic Reduction. *J. Phys. Chem. C* **2012,** *116*, 4809-4818.

(22) Goltl, F.; Love, A. M.; Hermans, I., Developing a Thermodynamic Model for the Interactions between Water and Cu in the Zeolite SSZ-13. *J. Phys. Chem. C* **2017,** *121*, 6160-6169.

(23) Paolucci, C.; Khurana, I.; Parekh, A. A.; Li, S.; Shih, A. J.; Li, H.; Di Iorio, J. R.; Albarracin-Caballero, J. D.; Yezerets, A.; Miller, J. T.; Delgass, W. N.; Ribeiro, F. H.; Schneider, W. F.; Gounder, R., Dynamic multinuclear sites formed by mobilized copper ions in NOx selective catalytic reduction. *Science* **2017,** *357* (6354), 898-903.

(24) Paolucci, C.; Parekh, A. A.; Khurana, I.; Di Iorio, J. R.; Li, H.; Albarracin Caballero, J. D.; Shih, A. J.; Anggara, T.; Delgass, W. N.; Miller, J. T.; Ribeiro, F. H.; Gounder, R.; Schneider, W. F., Catalysis in a Cage: Condition-Dependent Speciation and Dynamics of Exchanged Cu Cations in SSZ-13 Zeolites. *J. Am. Chem. Soc.* **2016,** *138*, 6028-6048.

(25) Paolucci, C.; Verma, A. A.; Bates, S. A.; Kispersky, V. F.; Miller, J. T.; Gounder, R.; Delgass, W. N.; Ribeiro, F. H.; Schneider, W. F., Isolation of the Copper Redox Steps in the Standard Selective Catalytic Reduction on Cu-SSZ-13. *Angew. Chem., Int. Ed.* **2014,** *53*, 11828-11833.

(26) Martini, A.; Borfecchia, E.; Lomachenko, K. A.; Pankin, I. A.; Negri, C.; Berlier, G.; Beato, P.; Falsig, H.; Bordiga, S.; Lamberti, C., Composition-driven Cu-speciation and reducibility in Cu-CHA zeolite catalysts: a multivariate XAS/FTIR approach to complexity. *Chem. Sci.* **2017,** *8*, 6836-6851.

(27) Goltl, F.; Sautet, P.; Hermans, I., The impact of finite temperature on the coordination of Cu cations in the zeolite SSZ-13. *Catal. Today* **2016,** *267*, 41-46.

(28) Li, H.; Paolucci, C.; Schneider, W. F., Zeolite Adsorption Free Energies from ab Initio Potentials of Mean Force. *J. Chem. Theory Comput.* **2018,** *14*, 929-938.

(29) Moreno-Gonzalez, M.; Hueso, B.; Boronat, M.; Blasco, T.; Corma, A., Ammonia-Containing Species Formed in Cu-Chabazite As Per In Situ EPR, Solid-State NMR, and DFT Calculations. *J. Phys. Chem. Lett.* **2015,** *6*, 1011-1017.

(30) Herr, J. D.; Steele, R. P., Signatures of Size-Dependent Structural Patterns in Hydrated Copper(I) Clusters, Cu+(H2O)n=1-10. *J. Phys. Chem. A* **2016,** *120*, 10252-10263.

(31) Kispersky, V. F.; Kropf, A. J.; Ribeiro, F. H.; Miller, J. T., Low absorption vitreous carbon reactors for operando XAS: a case study on Cu/Zeolites for selective catalytic reduction of NO(x) by NH3. *Phys Chem Chem Phys* **2012,** *14*, 2229-38.

(32) Kerkeni, B.; Berthout, D.; Berthomieu, D.; Doronkin, D. E.; Casapu, M.; Grunwaldt, J. D.; Chizallet, C., Copper Coordination to Water and Ammonia in CuII-Exchanged SSZ-13: Atomistic Insights from DFT Calculations and in Situ XAS Experiments. *J. Phys. Chem. C* **2018,** *122*, 16741-16755.

(33) Calligaris, M.; Nardin, G., Cation site location in hydrated chabazites. Crystal structure of barium- and cadmium- exchanged chabazites. *Zeolites* **1982,** *2*, 200.

(34) Calligaris, M.; Nardin, G.; Randaccio, L., Cation site location in hydrated chabazites. Crystal structure of potassium- and silver- excahnged chabazites. *Zeolites* **1983,** *3*, 205.

(35) Becke, A. D., A new mixing of Hartree-Fock and local-density-functional theories. *J. Chem. Phys.* **1993,** *98* (2), 1372-7.

(36) Lee, C.; Yang, W.; Parr, R. G., Development of the Colle-Salvetti correlation-energy formula into a functional of the electron density. *Phys. Rev. B: Condens. Matter* **1988,** *37* (2), 785-9.

(37) Dovesi, R.; Saunders, V. R.; Roetti, C.; Orlando, R.; Zicovich-Wilson, C. M.; Pascale, F.; Civalleri, B.; Doll, K.; Harrison, N. M.; Bush, I. J.; Arco, P. D.; Llunell, M. *CRYSTAL09 Users Manual, University of Turin: Turin, 2009, see http://www.crystal.unito.it.*, 2009.

(38) Dovesi, R.; Orlando, R.; Erba, A.; Zicovich-Wilson, C. M.; Civalleri, B.; Casassa, S.; Maschio, L.; Ferrabone, M.; De La Pierre, M.; D'Arco, P.; Noel, Y.; M., C.; Rerat, M.; Kirtman, B., Int. J. Quantum Chem., 2014, 114, . **2014,** *114*, 1287-1317.

(39) Ducere, J.-M.; Goursot, A.; Berthomieu, D., Comparative density functional theory study of the binding of ligands to Cu+ and Cu2+: Influence of the coordination and oxidation state. *J Phys Chem A* **2005,** *109* (2), 400-8.

(40) Civalleri, B.; Zicovich-Wilson, C. M.; Valenzano, L.; Ugliengo, P., B3LYP augmented with an empirical dispersion term (B3LYP-D*) as applied to molecular crystals. *CrystEngComm* **2008,** *10*, 405-410.

(41) Grimme, S., Accurate description of van der Waals complexes by density functional theory including empirical corrections. *J. Comput. Chem.* **2004,** *25*, 1463-1473.

(42) Boys, S. F.; Bernardi, F., The calculation of small molecular interactions by the differences of separate total energies. Some procedures with reduced errors. *Mol. Phys.* **1970,** *19* , 553-566.

(43) Cramer, C. J., *Essentials of Computational Chemistry: Theories and Models*. John Wiley & Sons Ltd: 2002; p 562 pp.

(44) Doronkin, D. E.; Casapu, M.; Guenter, T.; Mueller, O.; Frahm, R.; Grunwaldt, J.-D., Operando Spatially- and Time-Resolved XAS Study on Zeolite Catalysts for Selective Catalytic Reduction of NOx by NH3. *J. Phys. Chem. C* **2014,** *118*, 10204-10212.

(45) Goeltl, F.; Hafner, J., Structure and properties of metal-exchanged zeolites studied using gradient-corrected and hybrid functionals. II. Electronic structure and photoluminescence spectra. *J.Chem. Phys.* **2012,** *136* (6),

(46) Perez-Badell, Y.; Solans-Monfort, X.; Sodupe, M.; Montero, L. A., A DFT periodic study on the interaction between O-2 and cation exchanged chabazite MCHA (M = H+, Na+ or Cu+): effects in the triplet-singlet energy gap. *Physical Chemistry Chemical Physics* **2010,** *12* (2), 442-452.

(47) Berthomieu, D.; Jardillier, N.; Delahay, G.; Coq, B.; Goursot, A., Experimental and theoretical approaches to the study of TMI-zeolite (TM=Fe, Co, Cu). *Catal. Today* **2005,** *110* (3-4), 294-302.

(48) Jardillier, N.; Berthomieu, D.; Goursot, A.; Reveles, J. U.; Koster Andreas, M., Theoretical study of Cu(I)Y zeolite: structure and electronic properties. *J Phys Chem B.* **2006,** *110* (37), 18440-6.

(49) Chen, L.; Falsig, H.; Janssens, T. V. W.; Groenbeck, H., Activation of oxygen on (NH3-Cu-NH3)+ in NH3-SCR over Cu-CHA. *J. Catal.* **2018,** *358*, 179-186.